Bright Line Detection in COSMO-SkyMed SAR Images of Urban Areas

P.T.B. Brett and R. Guida
Surrey Space Centre
University of Surrey
Guildford, UK
p.brett@surrey.ac.uk

***Abstract*— Bright lines are a characteristic feature of synthetic aperture radar (SAR) amplitude images of urban areas, and are commonly associated with man-made structures. In order to aid in the development of SAR applications using these features, an automated approach to bright line detection is proposed, based on scale-space ridge detection at a single scale, and using a naïve Bayesian classification step to select the ridge points corresponding to bright lines. The effectiveness of the technique is demonstrated by applying it to a COSMO-SkyMed image of L'Aquila, Italy.**

I. Introduction

The launches of the COSMO-SkyMed constellation and the TerraSAR-X mission have made very high resolution Synthetic Aperture Radar (SAR) data widely available for civilian remote sensing applications, greatly increasing the level of detail visible in SAR images of urban areas.

A characteristic feature of metre-resolution SAR amplitude images of urban areas are bright, narrow lines, which arise from the geometry of man-made structures. For example, bright lines can be caused by direct specular scattering from surfaces normal to the sensor's look vector, such as gabled roofs, or by multiple-reflection scattering from two or more adjacent and mutually perpendicular surfaces, such as a building's wall and an adjacent paved road. Optical models have been developed for the analysis and simulation of building backscatter [1], and these have been inverted and applied to double-reflection lines manually extracted from SAR images in order to estimate parameters such as building height [2]–[4].

In order to make it easier to take advantage of bright line features in urban SAR image interpretation, an automated method for identifying points in a SAR image that lie on bright lines was desired.

A previous family of methods which are widely-used for detecting linear features in SAR images are based on the Hough transform [5], [6]. The Hough transform requires an expensive optimisation step, and does not cope efficiently with large-area images containing many short, disjoint lines.

Another family of common techniques for this task are those based on directional filtering [7], [8]. These have the drawback that line angle resolution is limited by the number of directional filter kernels used.

This paper presents a novel approach to bright line extraction based on direct ridge point detection (described in Sec. II) and subsequent classification of detected ridge points in order to remove dim and/or weak lines (Sec. III). It includes the results of applying the method to a SAR amplitude image from COSMO-SkyMed (Sec. IV).

II. Ridge point detection

A. Height definition for ridge points

The detection of bright lines in a SAR image is an application of *ridge detection.* There are a large number of different definitions of a 'ridge' (an overview of many of the more common ones is provided by [9]) and it is therefore necessary to clarify that the ridge detection method described in this paper is based on the *height definition* for a ridge. Let $f : \mathbb{R}^2 \rightarrow \mathbb{R}_+$ be a SAR amplitude image. Define the negated Hessian matrix of f, $W = -\mathrm{Hess}\,(f)$, and let k_1, k_2 and $\boldsymbol{\nu}_1, \boldsymbol{\nu}_2$ be its eigenvalues and eigenvectors, ordered such that $|k_1| \geq |k_2|$. Then a point in the image $\boldsymbol{x}$ is a *bright ridge point* if:

$$k_1 > 0 \quad \text{and} \quad \boldsymbol{\nu}_1^T \nabla f\,(\boldsymbol{x}) = 0. \tag{1}$$

B. Ridge detection in scale-space

Based on this height definition of a ridge point, [10] describes a scale-space approach to ridge detection. A brief summary of this method follows, in order to introduce terminology used later in this paper. The *scale-space representation* $L : \mathbb{R}^2 \times \mathbb{R}_+ \rightarrow \mathbb{R}$ of the image f is defined by $L\,(\boldsymbol{x}; t) = g\,(\boldsymbol{x}; t) * f$, where the scale parameter t is the variance of the Gaussian kernel $g : \mathbb{R}^2 \times \mathbb{R}_+ \rightarrow \mathbb{R}$. The *scale-space derivatives* are defined by $L_{x^\alpha y^\beta}\,(\boldsymbol{x}; t) = \partial_{x^\alpha y^\beta} L\,(\boldsymbol{x}; t)$, where (α, β) denotes the order of differentiation. At any image point $\boldsymbol{x}_0$ a local (p, q) coordinate system is defined, aligned with $\boldsymbol{\nu}_1, \boldsymbol{\nu}_2$, where W is formed from the second-order scale-space derivatives:

$$W\,(\boldsymbol{x}; t) = -\begin{bmatrix} L_{xx}\,(\boldsymbol{x}; t) & L_{xy}\,(\boldsymbol{x}; t) \\ L_{xy}\,(\boldsymbol{x}; t) & L_{yy}\,(\boldsymbol{x}; t) \end{bmatrix} \tag{2}$$

By analogy to (1), a point $\boldsymbol{x}_0$ is *bright ridge point of scale* t if:

$$L_{pp}\,(\boldsymbol{x}_0; t) < 0 \quad \text{and} \quad L_p\,(\boldsymbol{x}_0; t) = 0\ . \tag{3}$$

C. Adaptation to SAR urban bright line detection

Finite impulse response (FIR) filter approximations are used for g and the derivative operator ∂, and these are provided by the separable discrete scale-space (DSS) formulation proposed by [11]. Using these small, separable filters has the great advantage of allowing the scale-space to be computed quickly and efficiently.

Instead of extracting ridge segments as described in [10], the implementation described in this paper extracts only points. Once the ridge metrics L_{pp} and L_p have been computed, bright ridge points are found by first locating zero-crossing points of L_p by linear interpolation along rows and along columns, and then testing the sign of the corresponding interpolated value of L_{pp}. Each detected point therefore lies on the intersection of a bright line and the centreline of a row or column of pixels.

All three principle operations in the ridge detection process (i.e. DSS creation, eigendecomposition of W, and zero-crossing detection) can easily be carried out in parallel, permitting efficient multi-threaded implementation. This allows the ridge detection program to take full advantage of modern multicore CPU architectures, and ensures that the algorithm can easily scale to very large images.

A method is described in [10] for multi-scale ridge detection, whereby a normalised *ridge strength metric* $\mathcal{R}_{\mathrm{norm}}L$ is used to select the optimal scale for a ridge point. Unfortunately, for a typical SAR image (with size of order 10^8 pixels), prohibitively large amounts of memory are required for the creation of the scale-space and ridge metrics. Instead, the approach presented in this paper is based on carrying out ridge extraction at a single characteristic scale t_c. The development of an efficient multi-scale approach is a problem currently under study.

III. Ridge point classification

Ridge point detection detects both strong ridges (e.g. double-reflection lines) and weaker ones (e.g. arising from random noise in the image). A classification step allows ridge points that are of interest to be distinguished from those that are not. In this paper, a naïve Bayes classifier [12] is used to classify each detected ridge point $\boldsymbol{x}$. Two mutually-exclusive classes B and $\overline{B}$ are defined ('bright line' and 'not bright line' respectively), with two feature variables.

The first feature variable R_1 is the linearly-interpolated SAR backscattering amplitude at $\boldsymbol{x}$, i.e. $r_1 = f(\boldsymbol{x})$. It is modelled by a $\mathcal{G}_A^0$ distribution, $R_1 \sim \mathcal{G}_A^0(\alpha, \gamma, n)$, which has been demonstrated by to be a viable model for highly heterogeneous urban scatterers [13], [14]. The estimated parameters $\hat{\boldsymbol{\theta}}_1 = \{\hat{\alpha}, \hat{\gamma}, \hat{n}\}$ are derived from the training data using the log-moment method described in [14].

The second feature variable R_2 is the the *γ-normalised square principle curvature difference* $r_2 = \mathcal{N}_{\gamma-\mathrm{norm}}L(\boldsymbol{x})$ [10], a measure of ridge strength at $\boldsymbol{x}$, where

$$\begin{aligned}\mathcal{N}_{\gamma-\mathrm{norm}}L = \; & t^{4\gamma}\left(L_{xx}+L_{yy}\right)^2 \times \\ & \left(\left(L_{xx}-L_{yy}\right)^2 + 4L_{xy}^2\right).\end{aligned} \tag{4}$$

The authors propose to model the distribution of R_2 by the log-normal distribution $R_2 \sim \ln N\left(\mu, \sigma^2\right)$, and to use the *maximum a posteriori* (MAP) parameter estimates $\hat{\boldsymbol{\theta}}_2 = \{\hat{\mu}, \hat{\sigma}\}$ from the training data.

The MAP decision rule is used to determine into which class a ridge point $\boldsymbol{x}$ should be placed:

$$\ln\frac{p(B)}{p\left(\overline{B}\right)} + \sum_{i=1}^{2}\ln\frac{p\left(r_i\left(\boldsymbol{x}\right)|B\right)}{p\left(r_i\left(\boldsymbol{x}\right)|\overline{B}\right)} \underset{\overline{B}}{\overset{B}{\gtrless}} 0. \tag{5}$$

This approach allows both the 'brightness' and the 'sharpness' of a ridge to be taken into account in the classification.

IV. Results

The ridge detection and ridge point removal algorithms were tested by applying them to a single-look SAR amplitude image of L'Aquila, Italy, acquired by the COSMO-SkyMed constellation on 22nd March 2009. The image has an azimuth and range resolution of 0.8 m. The authors have not yet been able to obtain ground truth data for the target area for validation of results.

A. Estimation of t_c

First, a characteristic scale t_c to be used for ridge point detection was determined. A sample set of $N = 70$ bright line points $\{\boldsymbol{x}_i\}$ in the SAR image were manually identified, and the corresponding optimal scales

$$t_{\mathrm{opt},i} = \arg\max_t \mathcal{N}_{\gamma-\mathrm{norm}}L(\boldsymbol{x}_i, t) \tag{6}$$

were found. t_c was chosen as the mean of t_{opt}, rounded to the nearest $1/3$. The value found was $t_c = 3\,1/3$.

B. L'Aquila barracks

A military barracks in the northwest of L'Aquila was chosen as a target site for training the classifier. The site has two properties that make it suitable:

- Well-separated buildings, reducing the problems of layover and shadow.
- Buildings with relatively simple geometry, providing a variety of well-defined bright lines.

A 256×256 pixel SAR amplitude image segment containing the barracks is shown in Fig. 1a. The 17510 ridge points detected with $t_c = 3\,1/3$ were classified using a supervised process, as shown in Fig. 1b, and this classification was used to train the Bayesian classifier. The estimated parameters are shown in Table I, and the training data histograms and corresponding estimated probability density functions (PDFs) are shown in Fig. 2.

To verify the classifier, it was used to classify the ridge points of the training image (Fig 1c and Fig. 1d). The Bayesian classifier classified 9.80% of the ridge points differently to the supervised classification (7.16% false alarms and 2.65% misses). A qualitative assessment of the results suggested that the high false alarm rate was due to the Bayesian classification *correctly* classifying bright lines that had been omitted from the supervised classification.

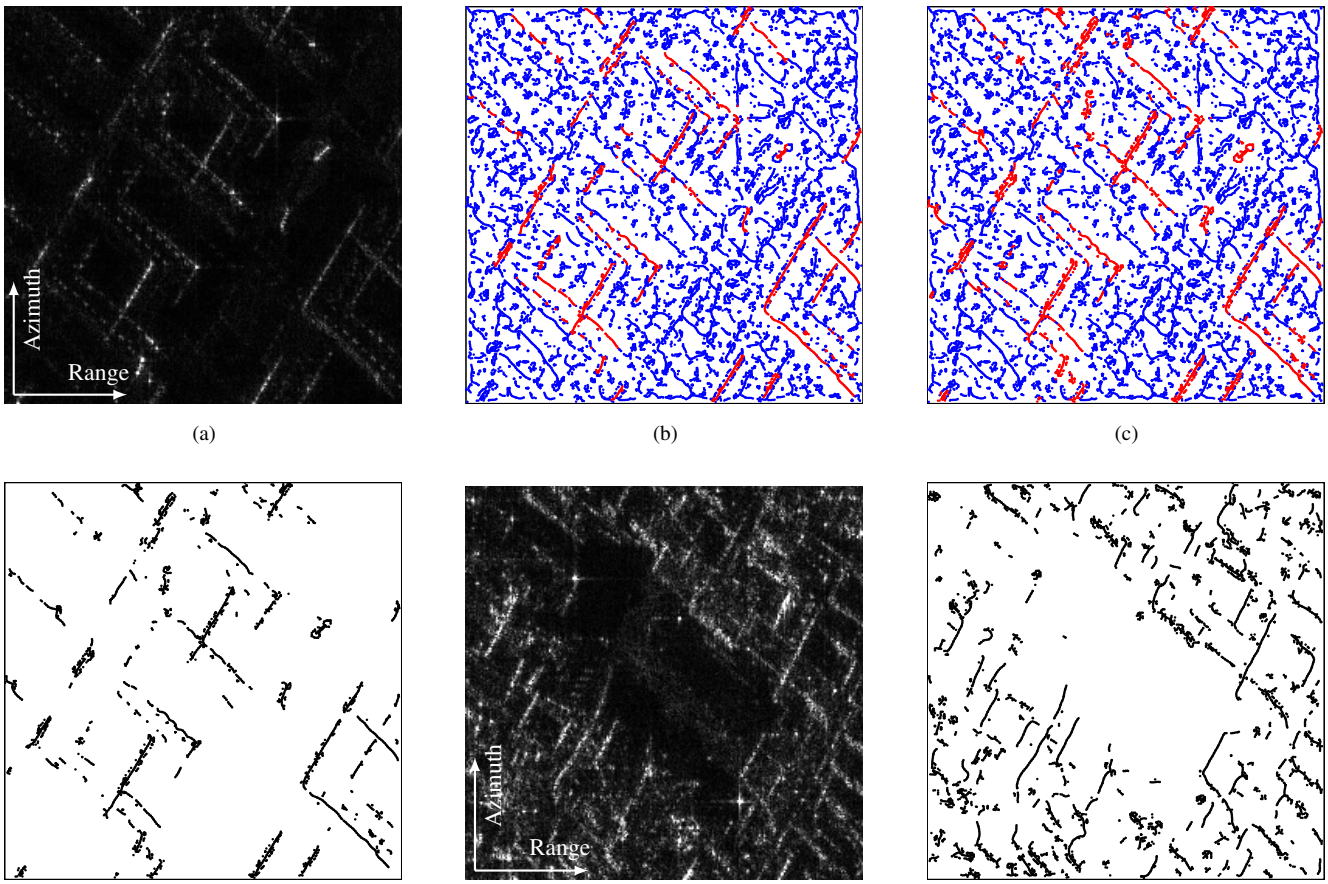

Fig. 1: L'Aquila bright line detection results. B is shown in red, and $\overline{B}$ in blue. Barracks: (a) original image, (b) supervised classification of detected ridge points, (c) Bayesian classification of detected ridge points, (d) Bayesian classification of detected ridge points (B only). Piazza del Duomo: (e) original image, (f) detected bright line points. Processed from COSMO-SkyMed product © Agenzia Spaziale Italiana 2009. All rights reserved.

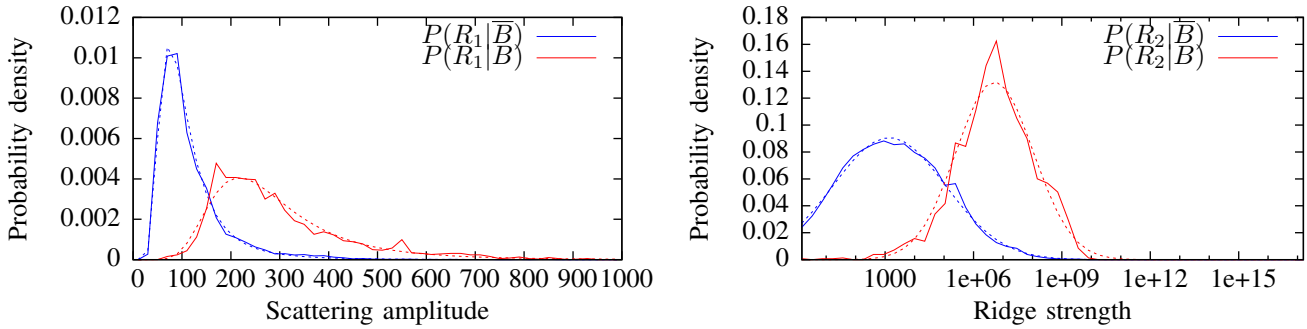

Fig. 2: MAP probability distributions of R_1 and R_2 after training. The training data histogram is plotted with lines, and the estimated feature models with dashes.

Feature	$R_1 \sim \mathcal{G}_A^0(\alpha, \gamma, n)$			$R_2 \sim \ln N(\mu, \sigma^2)$	
Parameter	$\hat{\alpha}$	$\hat{\gamma}$	$\hat{n}$	$\hat{\mu}$	$\hat{\sigma}$
B	-2.25	1.45×10^5	4.90	15.5	3.02
$\overline{B}$	-1.64	1.29×10^4	6.72	7.24	4.40
$p(B)$			0.12		

TABLE I: Estimated parameters for Bayesian classifier.

C. L'Aquila Piazza del Duomo

The trained classifier was then used to classify ridge points detected with the same $t_c = 3^1/_3$ in a segment of the SAR image covering the cathedral square (Piazza del Duomo) in the 'old town' area of L'Aquila (Fig. 1e). This area of the image contains very densely-packed buildings and a very heterogeneous environment, with strong overlay and shadow effects in evidence, making manual extraction of bright lines challenging. Fig. 1f shows the bright line points detected using the Bayesian classifier. Note in particular the clarity with which the overlay of the building on the south-east edge of the square has been picked out, and that bright lines have been successfully extracted from high-noise areas (e.g. along the north edge of the square).

V. Conclusion

A new approach to the detection of bright lines in very high-resolution single-look urban SAR images is proposed, including the novel application of scale-space ridge detection to SAR data using a single characteristic scale. A classification step based on the naïve Bayes classifier is proposed for selection of the ridge points corresponding to bright lines, and suitable feature variables and corresponding statistical models are suggested. The technique is demonstrated by applying it to a single-look COSMO-SkyMed SAR amplitude image of L'Aquila, Italy.

The technique improves on established methods for SAR image linear feature detection, providing both greater scalability than Hough transform methods and single-step detection of bright lines at any orientation.

The problem of distinguishing between bright lines due to direct and double-reflection scattering is currently under study, and more extensive testing is to be carried out both on other SAR images and on other parts of the L'Aquila dataset. Additionally, the potential application of automatic bright line extraction to urban change detection is being explored.

Acknowledgments

The authors would like to thank the Remote Sensing Group at the University of Naples Federico II and the Italian Space Agency for providing the COSMO-SkyMed SAR images used in this study, and the UK Engineering and Physical Sciences Research Council (EPSRC) for funding the research project.

References

[1] G. Franceschetti, A. Iodice, and D. Riccio. A canonical problem in electromagnetic backscattering from buildings. *Geoscience and Remote Sensing, IEEE Transactions on*, 40(8):1787–1801, Aug. 2002.

[2] G. Franceschetti, R. Guida, A. Iodice, D. Riccio, G. Ruello, and U. Stilla. Building feature extraction via a deterministic approach: application to real high resolution SAR images. In *Geoscience and Remote Sensing Symposium, 2007. IGARSS 2007. IEEE International*, pages 2681–2684, July 2007.

[3] R. Guida, A. Iodice, and D. Riccio. Assessment of TerraSAR-X products with a new feature extraction application: Monitoring of cylindrical tanks. *Geoscience and Remote Sensing, IEEE Transactions on*, 48(2):930–938, Feb. 2010.

[4] R. Guida, A. Iodice, and D. Riccio. Height retrieval of isolated buildings from single high-resolution SAR images. *Geoscience and Remote Sensing, IEEE Transactions on*, 48(7):2967–2979, July 2010.

[5] J.W. Wood. Line finding algorithms for SAR. Royal Signals and Radar Establishment, Memo. 3841, 1985.

[6] N. Aggarwal and W.C. Karl. Line detection in images through regularized Hough transform. *Image Processing, IEEE Transactions on*, 15(3):582–591, Mar. 2006.

[7] F. Tupin, H. Maître, J.-F. Mangin, J.-M. Nicolas, and E. Pechersky. Detection of linear features in SAR images: application to road network extraction. *Geoscience and Remote Sensing, IEEE Transactions on*, 36(2):434–453, Mar. 1998.

[8] P. Gamba, F. Dell'Acqua, and G. Lisini. Improving urban road extraction in high-resolution images exploiting directional filtering, perceptual grouping, and simple topological concepts. *Geoscience and Remote Sensing Letters, IEEE*, 3(3):387–391, july 2006.

[9] D. Eberly, R. Gardner, B. Morse, S. Pizer, and C. Scharlach. Ridges for image analysis. *Journal of Mathematical Imaging and Vision*, 4(4):353–373, 1994.

[10] T. Lindeberg. Edge detection and ridge detection with automatic scale selection. *International Journal of Computer Vision*, 30(2):117–154, 1998.

[11] J.Y. Lim and H.S. Stiehl. A generalized discrete scale-space formulation for 2-D and 3-D signals. *Scale Space Methods in Computer Vision*, pages 132–147, 2003.

[12] David Lewis. Naïve (Bayes) at forty: The independence assumption in information retrieval. In Claire Nédellec and Céline Rouveirol, editors, *Machine Learning: ECML-98*, volume 1398 of *Lecture Notes in Computer Science*, pages 4–15. Springer Berlin / Heidelberg, 1998.

[13] A.C. Frery, H.-J. Muller, C.C.F. Yanasse, and S.J.S. Sant'Anna. A model for extremely heterogeneous clutter. *Geoscience and Remote Sensing, IEEE Transactions on*, 35(3):648–659, May 1997.

[14] C. Tison, J.-M. Nicolas, F. Tupin, and H. Maître. A new statistical model for Markovian classification of urban areas in high-resolution SAR images. *Geoscience and Remote Sensing, IEEE Transactions on*, 42(10):2046–2057, Oct. 2004.